Applied Geochemistry 93 (2018) 145–157

Contents lists available at ScienceDirect

Applied Geochemistry

journal homepage: www.elsevier.com/locate/apgeochem

Characterization of a gold extraction plant environment in assessing the hazardous nature of accumulated wastes (Kemerovo region, Russia)

Svetlana Bortnikova[a], Vladimir Olenchenko[a], Olga Gaskova[b,c], Nataliya Yurkevich[a,c,d], Natalya Abrosimova[a], Elizaveta Shevko[b], Aleksey Edelev[a,*], Tatyana Korneeva[a], Irina Provornaya[a,c], Leontiy Eder[a,c]

[a] *Trofimuk Institute of Petroleum Geology and Geophysics, Siberian Branch of the Russian Academy of Sciences, Koptug Ave. 3, 630090 Novosibirsk, Russia*
[b] *Sobolev Institute of Geology and Mineralogy, Siberian Branch of the Russian Academy of Sciences, Koptug Ave. 3, 630090 Novosibirsk, Russia*
[c] *Novosibirsk State University, Pirogova St. 2, 630090 Novosibirsk, Russia*
[d] *Novosibirsk State Technical University, K. Marksa Ave. 20, 630073 Novosibirsk, Russia*

ARTICLE INFO

Handling Editor: Michael Kersten.

Keywords:
Arsenic
Komsomolsk tailings
Environmental pollution assessment
Electrical resistivity tomography
Economic evaluation

ABSTRACT

Geochemical and geophysical investigations were performed in the area of the Komsomolsk tailings impoundment. Gold ore tailings produced with cyanidation have been generated by the Komsomolsk Gold Extraction Plant. The relatively low sulfide content in the Komsomolsk tailings and the presence of carbonates result in a low acid production potential (AP) for these tailings. The tailings pond is characterized by neutral to slightly alkaline conditions and metal concentrations, except for those of As and Sb, below the maximum permissible concentration (MPC). The situation is complicated by the fact that the displaced Berikul tailings are stored in the southern part of the Komsomolsk tailings impoundment. Sulfide concentrate cyanidation tailings were produced by the former Berikul Gold Extraction Plant. In the Berikul tailings, the sulfide content is approximately 25%. This high content has resulted in a high AP and the formation of acidic and ultra-acidic surface ponds (pH ~2) with extremely high concentrations of metals and metalloids (As up to 4.1 $g\,L^{-1}$). The estimated duration of acid drainage generated by the Berikul tailings is approximately 2400 years. Surface drainage from the tailings enters the Voskresenka River; as a result, the concentrations of As and Sb in the river water approach the MPCs established by the Russian Ministry of Health. Based on electrical resistivity tomography (ERT), the uncontrolled leakage of acidic and highly mineralized solutions through a natural geological fault into groundwater horizons was revealed. Groundwater contamination was confirmed via an analysis of drinking water from a well located near the fault.

1. Introduction

The migration of chemical elements, especially As, Sb, Cu, Zn, Cd, and Pb, from mine tailings and waste has been widely investigated. High contents exceeding the maximum permissible concentrations (MPCs) of metals and metalloids in drainage and surface mine waters have been observed in many abandoned and active mining areas worldwide (Edraki et al., 2005; Meck et al., 2006; Cravotta, 2008; Cidu et al., 2013). Since the 20th century, there has been a significant focus on the geochemistry of acid mine drainage (AMD) and its impact on the environment. Many investigations have described the geochemical and mineralogical compositions of mine tailings and surface mine waters, as well as AMD geochemistry (Paktunc et al., 2003, 2004; Wang and Mulligan, 2006; Lottermoser, 2010; Blowes et al., 2014; Martin-Crespo et al., 2015; Korneeva et al., 2017). Over the past decade, considerable research has focused on understanding mine drainage generation and minimizing the associated effects on the environments.

There is a clear need to develop a more comprehensive approach for evaluating the environmental hazards associated with the release of metals and metalloids to the environment (Bortnikova et al., 2006; Gas'kova et al., 2008; Tolaymat et al., 2015). This approach should cover a wide range of processes that determine the fate of toxic elements in mining regions (Bortnikova et al., 2003). Monitoring of man-made lakes (tailings impoundment) or waste heaps using a combination of geochemical and geophysical methods can serve as a basis for developing a quantitative model of toxic element behavior in various

---

[*] Corresponding author.

E-mail addresses: BortnikovaSB@ipgg.sbras.ru (S. Bortnikova), OlenchenkoVV@ipgg.sbras.ru (V. Olenchenko), Gaskova@igm.nsc.ru (O. Gaskova), YurkevichNV@ipgg.sbras.ru (N. Yurkevich), AbrosimovaNA@ipgg.sbras.ru (N. Abrosimova), Liza@igm.sbras.ru (E. Shevko), EdelevAV@ipgg.sbras.ru (A. Edelev), KorneevaTV@ipgg.sbras.ru (T. Korneeva), ProvornayaIV@ipgg.sbras.ru (I. Provornaya), EderLV@ipgg.sbras.ru (L. Eder).

https://doi.org/10.1016/j.apgeochem.2018.04.009
Received 29 November 2017; Received in revised form 12 April 2018; Accepted 21 April 2018

environmental compartments (lakes, pore water, silt solutions, bottom sediments buried tailings, etc.).

In the past fifty years, the numbers of studies of remediation in areas affected by mining activities and assessments of the influence of waste on the environment have significantly increased. Currently, most investigations of mine tailing areas are conducted using geophysical methods to determine the mine drainage distribution in a given coordinate space (Martín-Crespo et al., 2010; Placencia-Gómez et al., 2010; Martínez-Pagán et al., 2011; Martínez et al., 2012, 2016; Zarroca et al., 2015; Tycholiz et al., 2016; Olenchenko et al., 2016; Yurkevich et al., 2015, 2017a; 2017b) and trace the paths of toxic elements in mine waste (Kazakis et al., 2017).

Special attention has been given to the behavior, transport and deposition of arsenic as a particularly toxic element. Studies of arsenic toxicology and the associated hazards are closely associated with the development of available technologies for arsenic removal (Mondal et al., 2006; Choong et al., 2007; Fan et al., 2016; Cheng et al., 2017).

Various aspects of arsenic transport from stored tailings into the environment have been studied for many years and include the oxidation of sulfide- and As-bearing tailings (Bowell and Bruce, 1995; Blowes et al., 1998; Courtin-Nomade et al., 2003; Bodénan et al., 2004), arsenic modes of occurrence in tailings and the soil (Cullen and Reimer, 1989; Foster et al., 1998; Roussel et al., 2000; Savage et al., 2000; Bortnikova et al., 2010, 2012), and secondary As minerals in contaminated soil and waste systems (Drahota and Filippi, 2009).

New experimental simulations have been performed on the release of metals (Cu, Pb, Zn) and metalloids (As, Sb) from mine tailings (Paktunc et al., 2003; Walker et al., 2006; Abrosimova et al., 2015a) and their subsequent adsorption on formed iron hydroxides (Fuller et al., 1993; El Adnani et al., 2016; Hiller et al., 2016) in addition to studies of As behavior in soil (Dousova et al., 2012) and in As-rich tailing profiles (Armienta et al., 2012), metalloids intake by plants from contaminated soils (Cidu et al., 2014; Simmler et al., 2016) and accumulation in organic-bearing material can be used for remediation of polluted areas as well as for secondary enrichment technologies (Saryg-ool et al., 2017).

The arsenic limit in drinking water and reservoirs for domestic use recommended by the World Health Organization (WHO) and Russian Ministry of Health is 10 μg L^{-1} (WHO, 2011; RMH, 2003). However, an As concentration of approximately 10 μg L^{-1} may still cause cancer (Quansah et al., 2015).

Current information regarding the area near the Komsomolsk tailings impoundment after the undigested placement of the Berikul tailings is not publicly available. Therefore, a relevant assessment with conclusions and practical recommendations should be submitted to the administration of the Kemerovo region. A science-based approach for environmental monitoring could provide a simultaneous assessment of the economic feasibility of the extraction of valuable tailings components.

The objectives of this article are as follows: 1) present new surface and groundwater composition data from two contrasting tailings sites; 2) perform an electrical resistivity tomography (ERT) survey to evaluate the volume of tailings in the impoundment; 3) determine the spreading direction of contaminated waters in the area of the Komsomolsk tailings impoundment; 4) provide a science-based approach for monitoring and protecting groundwater resources that can be applied in other mine-impacted areas; and 5) estimate the environmental damage to polluted waters and assess the economic feasibility of extracting valuable components from the tailings.

2. Study area

The Komsomolsk gold deposit is located in the Eastern Kemerovo region, Russia. It is a system of gold-arsenopyrite-quartz veins with a large stock of gabbroids. The deposit was mined from 1937 to 1999. The primary sulfide minerals are pyrite, pyrrhotite, and arsenopyrite with lower contents of galena, sphalerite, and chalcopyrite (2–2.5% of the total deposit). Quartz, feldspar, and mica are the most abundant gangue minerals, and some carbonate grains (calcite and dolomite) are present (~6%). The ores of the Komsomolsk deposit were processed using cyanidation techniques with NaCN at the Komsomolsk Gold Extraction Plant (KGEP). Gold precipitation was performed with zinc dust, and the main product was Au sludge. In addition, KGEP produced gold extracted from the antimony sludge (the remaining product after leaching antimonite concentrates using Na_2S and NaOH) of the Kadamjai Plant. This sludge constituted a small portion of the mine waste (0.5 tons of sludge was added to every 100 tons of ore) but was rich in metal contents.

The KGEP tailings are located in the territory of the Komsomolsk settlement and 1 km to the northeast of the plant (Fig. 1S in Supplementary Material). The tailings have been present since 1964. The tailings impoundment is a natural ravine filled with slurry runoff. The tailings area is 146,000 m^2, and the amount of solid accumulated material is ≈ 1.1 million m^3, or 3.5 million tons. The impoundment is topographically enclosed on three sides and by a bulk dam on the fourth side. A tailings pond formed at the surface due to particle accumulation and consolidation. The pond area is ≈ 60,000 m^2, and the average depth is 2 m. Currently, the pond is primarily replenished by seasonal atmospheric precipitation. At times, the pond water flows under the dam to the surface and then enters the Voskresenka River. Descriptions of the mine tailings and mineralogical data were provided in previous works (Lazareva et al., 1999; Gas'kova et al., 2000; Shuvaeva et al., 2000). We should emphasize that the tailings impoundment is located near a living area in the Komsomolsk settlement. Recently, the population has perceived the water body as a “natural” pond, and it is actively used for domestic purposes (Fig. 2S (a) in Supplementary Material).

Additionally, after the cyanide leaching of sulfide flotation concentrate from the Berikul Gold Extracting Plant (BGEP), 100,000 tons of tailings was transported and stored in the southern portion of the tailings impoundment in 2004 (Fig. 1S in Supplementary Material). The Berikul gold mine was situated 20 km from Komsomolsk and exploited the gold-sulfide-quartz veins of the Staro-Berikul and Novo-Berikul deposits. The main ore minerals were quartz, calcite, pyrite, pyrrothite, arsenopyrite, and chalcopyrite. Sphalerite, galena, tennantite, tetrahedrite, dolomite, ankerite, gold, silver, burnonite, and bornite were minor minerals (Alabin and Kalinin, 1999). The mine was worked between 1942 and 1991, and ores were processed at the BGEP. According to BGEP archives, flotation concentrate was produced during primary processing. Additionally, gold was extracted from sulfides using cyanide-based techniques. After the removal of the Au-bearing cyanide solutions, the sulfide flotation residues were neutralized by adding $Ca(ClO)_2$ before being dumped onto waste piles. Previously, this waste was stored in bulk at the Old Berikul settlement (Gieré et al., 2003; Sidenko et al., 2005). Initially, there was a plan to extract gold from these tailings at the Komsomolsk Plant, but the lack of cost-effective technology and the high toxicity of the waste did not allow for the implementation of this plan. As a result, the Berikul tailings are stored in the southern part of the Komsomolsk tailings impoundment. The amount of solid accumulated material totals 100,000 tons. The discarded material contains more than 25% of fine-grained sulfides, including pyrite (35–40 wt%), arsenopyrite (2–5 wt.%), and minor amounts of pyrrhotite, sphalerite, chalcopyrite, and galena. Among the gangue minerals found in the waste, the predominant phases are quartz (30–35 wt%), albite (5–10 wt%), chlorite (5–10 wt%), and calcite (3–5 wt.%) (Gieré et al., 2003). Many secondary minerals have been described in the waste (Gieré et al., 2003; Sidenko et al., 2005). The ponds were formed by seasonal precipitation immediately on top of the displaced Berikul tailings (Fig. 2S (b) in Supplementary Material). The volume and configuration of the ponds seasonally changes. The pond water has a brownish-black to light red color. Interactions with highly oxidized tailings led to the formation of the current hydrochemical

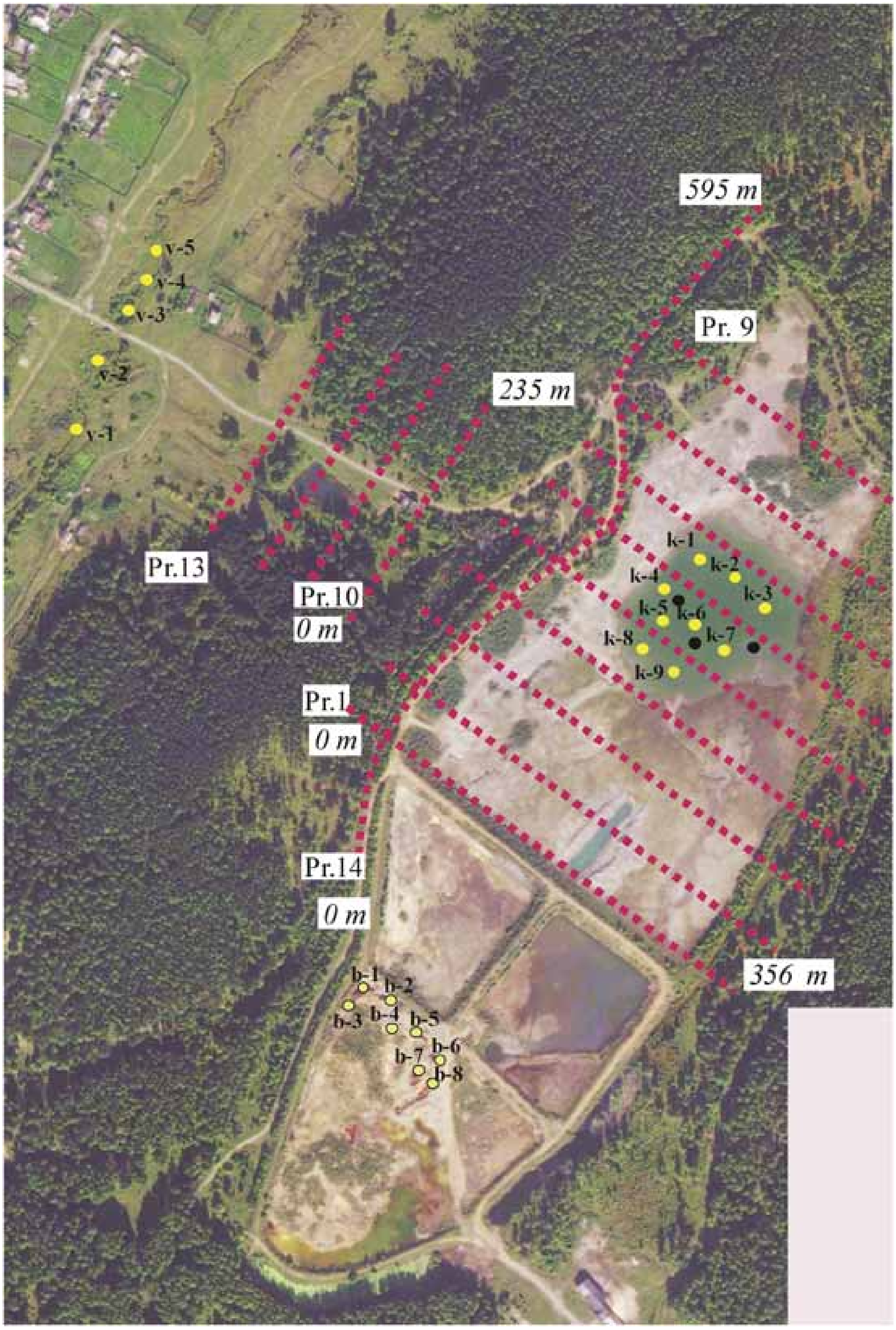

Fig. 1. Sample sites in the Komsomolsk area. Black points – cores of sediments; yellow points – water samples; red dotted lines – ERT profiles. (For interpretation of the references to color in this figure legend, the reader is referred to the Web version of this article.)

composition of the solutions. Drinking water for the settlement population is supplied from underground horizons at depths of 20–40 m through tubular wells, and the well locations are shown in Fig. 1S (Supplementary Material).

3. Methods

3.1. Field study

During field activities and laboratory work from 2014 to 2015, the

Komsomolsk tailings impoundment area was investigated with geochemical sampling and geophysical survey techniques. These studies supplemented earlier work conducted before Berikul tailings were dumped at the impoundment.

3.1.1. Sampling

To determine the composition of the tailings that interacted with pond water, three 30–60-cm deep sediment cores were extracted from the bottom of the Komsomolsk pond (black points, Fig. 1). Sampling was performed from a catamaran. Core columns were sliced and transferred into polyethylene bags for laboratory analyses (total of 44 samples).

Water was sampled from the Komsomolsk tailings pond, Berikul ponds on the tailings piles (two groups of red dots, Fig. 1), and the Voskresenka River. The samples were collected in plastic bottles rinsed with the sampled water. Drinking water wells were sampled at the locations shown in Fig. 1S (Supplementary Material). Water from B. Berchikul Lake was sampled to determine the regional hydrogeochemical background. B. Berchikul Lake is located 6 km from the Komsomolsk tailings impoundment in an area without any technogenic influence.

Water samples were divided into two sets. The first aliquot was filtered at the sampling site to < 0.25 μm using a microfiltration hydrophobic membrane (Vladipor, Russia). The second aliquot, which was reserved for anion analyses, was not filtered.

In the water samples, the pH value and redox potential (Eh) were measured in situ using a pH/temperature meter (HI 9025 C, Hanna Instruments, Italy), a combined glass electrode for pH (HI 1230 B, Hanna Instruments), and a Pt electrode for Eh (Oxidation Reduction Potential Electrode, Hanna Instruments) (Nordstrom, 1977). Electrical conductivity was determined using a Cond 315 i conductivity meter (WTW, USA). Neutral and subalkaline water samples were acidified with distilled HNO_3 (purity of 99%).

3.1.2. Geophysical investigation

ERT has been applied in fault, groundwater table, soil moisture content and various other investigations. ERT (Loke, 2000; Bobachev and Gorbunov, 2005) was performed using a multielectrode resistivity meter Skala-48 (IPGG SB RAS, Novosibirsk) (Balkov et al., 2012) for nine profiles to reveal the geoelectric structure of the local area to a depth of 30 m. The observation network included profiles No. 1–9 and comprised a total length of 356 m. In addition, a geophysical survey was performed along the drainage pathway system for four profiles (No. 10–13), with a length of 235 m, and a single profile (No. 14) on the dam, with a length of 595 m (Fig. 1). ERT was performed using a Schlumberger array. The distance between electrodes was 5 m. The depth of the investigation was 40 m. Data processing was performed using Res2Dinv and Res3Dinv software (Loke, 2000). Two-dimensional geoelectric sections and a three-dimensional model of the resistivity distribution in the environment were constructed using the processed data.

3.2. Laboratory analyses

3.2.1. Analytical methods for solid and water samples

The solid samples were dried at room temperature for 48 h and powdered to < 74 μm by abrasion in an agate mortar for bulk analysis. The silicate group oxide contents were determined via X-ray fluorescence analysis. Trace element concentrations in tailings were determined on 30-mg pressed pellets based on XRF with synchrotron radiation (Baryshev et al., 1986) at station VEPP-3 at the Institute of Nuclear Physics SB RAS, Novosibirsk, Russia. Measurements were made at an activation energy of 30 keV according to the method of internal standards. The resulting XRF spectra were processed with the AXIL IBM-PC V3.00 program. Quality assurance/control was performed for the data using replicate analyses of every 10th sample and standards. The accuracy and precision were estimated to be 10–15% or better at the $g \cdot t^{-1}$ concentration level.

The content of CO_2 in the solid tailings was determined by decompounding calcium and magnesium carbonates (calcite, dolomite, and ankerite) from 0.5-g sample batches in cold HCl solution (1:4), the absorption of isolated carbon dioxide by sodium hydroxide, the precipitation of carbonate ions in barium chloride solution, and the subsequent titration of free hydroxide ions using hydrochloric acid with a phenolphthalein indicator. The carbon dioxide concentration was calculated as the difference between the quantity of hydrochloric acid used for the titration of the sodium hydroxide solution before and after the absorption of carbon dioxide. State standard reference samples with carbon dioxide concentrations varying from 0.1 to 47% were used to verify test results.

The concentration of sulfide sulfur was calculated as $S_{total} - S_{sulphate}$. Each test batch was sintered in a kiln at 800°C with an Eschka mixture (200 g Na_2CO_3 and 400 g MgO). The sinter was transferred into a hot solution and boiled for 5 min. After filtration, it was acidified with HCl, precipitated as $BaSO_4$ by adding $BaCl_2$, and weighed.

Sulfate sulfur was determined in a batch of 0.5 g that was boiled in a 10% aqueous solution of HCl. After the solution was filtered and sulfate sulfur was precipitated by adding $BaCl_2$, the sulfate content was weighed.

In water samples, major cation (Al, Fe, Ca, Mg, K, Na, and Si) and trace element analyses were conducted using ICP-AES (IRIS Advantage) at the Analytical Center of IGM SB RAS. In the water analyses, each third sample was analyzed twice. The error in the ionic balance was less than 15%. Another aliquot was analyzed for major anions (SO_4^{2-}, Cl^-, HCO_3^-) using photometric and titrimetric methods. The accuracy and precision were estimated to be 7% or better at the mg L^{-1} concentration level.

3.2.2. Calculating the net acid potential

Comparative analysis of the acid generation potential (AP) and acid neutralization potential (NP) is widely used in mine drainage assessment (Abrosimova et al., 2015b; Bailey et al., 2015; Çelebi and Öncel, 2016; Qureshi et al., 2016; Wei et al., 2016; Kefeni et al., 2017; Balci and Demirel, 2018). Following the methods of Skousen et al. (2002) and Sobek et al. (1978), the AP was calculated from the content of sulfide sulfur (A) and measured as the amount of calcium carbonate (kg/ton) necessary for acid neutralization. Based on convention, the oxidation of 1 mol of sulfide sulfur yields 2 mol of hydrogen cations, which, in turn, are neutralized by 1 mol of carbonate.

$$AP = S_{sulfide}(wt\%) \times 31.25, \tag{A}$$

where 31.25 is a factor determined from the stoichiometry of reaction (B).

$$FeS_2 + 2CaCO_3 + 15/4O_2 + 7/2H_2O = Fe(OH)_{3(s)} + 2SO_4^{2-} + 2Ca^{2+} + 2H_2CO_{3(aq)} \tag{B}$$

This reaction indicates that 2 mol of calcite are used for every 2 mol of sulfur (1 mol of pyrite) in the complete reaction.

The NP is used to quantitatively estimate the capability of a substance to neutralize AMD water (Skousen et al., 2002; Sobek et al., 1978). The NP value is often calculated from the content of carbonate minerals in a substance. In this case, the NP values (kg $CaCO_3$/ton) (Paktunc, 1999) were calculated using the following standard formula (C):

$$\begin{aligned} NP &= 10 \times n(C) \times M(CaCO_3)/M(C) = 10 \times n(C) \times 100.09/12 \\ &= n(C) \times 83.41, \end{aligned} \tag{C}$$

where 10 is a coefficient used to convert kg/ton to wt.%; n (C) is the content of carbonate carbon in the substance in wt.%; and $M(CaCO_3)$ and M(C) are the molar masses of $CaCO_3$ (100.09 g/mole) and carbon (12 g/mol), respectively.

The difference between the AP and NP is the net acid potential (NAP): NAP = AP – NP (Sobek et al., 1978).

3.2.3. Calculating the species and saturation indices

Speciation-equilibrium calculations were performed using WATEQ4F (Ball and Nordstrom, 1991) with the included database. This program is generally used to calculate the speciation of dissolved ions in an aqueous solution and the saturation indices (SIs) of mineral phases as a function of the pH, temperature, composition and ionic strength of a solution. A positive SI value indicates that the mineral will precipitate, a negative SI value suggests that the mineral will dissolve, and a log SI value equal to ± 0.3 indicates equilibrium between the aqueous solution and mineral.

3.2.4. Economic evaluation of environmental impacts

In economic assessments of environmental damage, different proven and widely used methodological approaches have been applied. Specifically, the method of the Ministry of Natural Resources of the Russian Federation and other methods for evaluating the environmental damage caused by the discharge of pollutants into ponds (GR, 1999) have been used.

The environmental damage caused by the pollution of water resources (Y_B) was calculated in stages according to the following procedure:

$$Y_B = \gamma_B \cdot \sigma_B \cdot M_B, \tag{1}$$

where γ_B is an indicator of the damage (pollution price) to water resources caused by one ton of the reduced mass of pollutants at the end of the reporting period for a water body in the study region (USD/ton); σ_B is a coefficient of ecological importance for water bodies in the basin of major rivers; and M_B is the reduced mass of pollutants in the water during the reporting period (tons). The reduced mass (M_B) is calculated based on the total weight of discharged pollutant i (m_i) and the relative danger of substance i (A_i):

$$M_B = \sum_{i=0}^{N} A_i \cdot m_i, \tag{2}$$

where N is the total number of contaminants.

The indicator of the relative danger of substance i A_i is determined based on the MPCs (RMH, 2003) of chemical substances in water bodies for drinking and cultural and community water use.

$$A_i = \frac{1}{MPC_i} \tag{3}$$

The numerical value of the damage γ_B to water resources can be determined based on the value of the above parameter, as previously noted in the literature (Girusov et al., 2003).

4. Results and discussion

4.1. Composition of tailings

The main difference between the compositions of the Komsomolsk and Berikul tailings was the difference in the compositions of the processed substances. At the KGEP, ores with relatively low sulfide contents (2–5% of the total mass) were processed, and a substance that had been preliminarily concentrated by flotation was processed at Berikul. Moreover, the pond at the Komsomolsk tailings impoundment provides a protective screen from atmospheric gas penetration; therefore, sulfide minerals are protected from oxidation. In some outer portions of the tailings, the locally intense oxidation of minerals can be observed (Kirillov et al., 2016). In most samples of the Komsomolsk tailings, the average $S_{sulfide}$ content is approximately 2%, and the $S_{sulfate}$ content is not more than 0.7% (generally less than 0.01%; Table 1). The content of CO_2, which denotes the amount of carbonate in the tailings, varies from 1.9 to 4.5% and averages 3.2%.

Because gold extraction at the Berikul Plant was performed via the cyanidation of sulfide flotation concentrate, the $S_{sulfide}$ content in the Berikul tailings is significantly higher than that in the Komsomolsk tailings (Table 2). Notably, the $S_{sulfide}$ content is approximately 13.6%, and the $S_{sulfate}$ content is greater than 12.8%.

Fig. 4 exhibits the difference in the elemental compositions of the Komsomolsk and Berikul tailings. A line at a 45° angle separates the antimony-rich Komsomolsk tailings from the arsenic-rich Berikul tailings on the correlation plot (Fig. 3S in Supplementary Material). The Komsomolsk tailings are richer in rock-forming elements (Si, Al, and Ca are above the line), Sb and CO_2, but the Berikul tailings are richer in metals (Fe, Cd, Cu, Cr, Pb, Zn, and As are below the line) and S, which influence the specificity of the leaching solutions.

Fig. 2 presents the calculated values of NP and AP. Considering these values, it was assumed that the Berikul tailings produced acid leachates in the short and long terms because the average NAP is 415 kg $CaCO_3$/ton. Additionally, sulfuric acid that forms during the sulfide oxidation of the Komsomolsk tailings will be neutralized by carbonates (NP ~ AP). A high NAP value indicates a high probability for the localized formation of acid waters in the future (at some points where AP > NP).

Calculations were performed to assess the duration of acid drainage generation for the Berikul tailings. The following conditions were assumed in the calculations: 1) the limiting stage encompasses the flushing of water involved in the sulfide oxidation reaction; 2) the water inflow volume is estimated from the amount of annual precipitation and the area of the tailings; and 3) the pH of the drainage water is taken as 2. The area of the displaced tailings is approximately 70,000 m^2. The average annual rainfall in the Kemerovo region is 500 mm, and 35,000 m^3 or $35 \cdot 10^6$ L of water falls on the tailings surface per year. The mass of the tailings is 100,000 tons, and the amount of generated acid is ≈ 407 kg H_2SO_4 per ton of tailings. Accordingly, the net (total) quantity of acid is 41×10^6 kg H_2SO_4. The resultant pH of the drainage solution is approximately 2 based on the pH value of secondary sulfate dissolution (reactions 1–10). As a result, the volume of water associated with the calculated pH is 8.3×10^{10} L and, considering the inflow, equals 35×10^6 L per year. Thus, acid production in the Berikul tailings is expected to last for 2400 years.

4.2. Composition of pond waters

The net composition and physico-chemical parameters of the pond on the surface of the Komsomolsk tailings impoundment are the result of the continuous interactions of seasonal precipitation and solid tailings. The composition is stable in all analyzed samples, and it is characterized by a slightly alkaline or alkaline pH, oxidizing conditions and a relatively low total dissolved solids (TDS) level of 0.5 g L^{-1} (Table 3). Notably, these data are in good agreement with the results of past studies of the pond water (Gas'kova et al., 2000). Despite the low TDS level, the waters are SO_4^{2-}-Ca type, which is typical for technogenic ponds. The contents of most of the observed elements did not exceed the MPC (Table 3). The primary toxic elements are As and Sb, and the concentrations of both are relatively stable. Specifically, the As and Sb contents exceed the MPC (RMH, 2003) by factors of 21 and 170 on average, respectively.

The open ponds on the Berikul tailings contain acidic and ultra-acidic solutions. The solution compositions and physico-chemical parameters vary from pond to pond (Table 4). These solutions can be classified as unusual sulfate-arsenate-iron-aluminum-type solutions. The concentrations of all measured elements were many times higher than the MPC. It is impossible to determine which elements are the most dangerous; however, the concentration of aluminum (a 3rd-class danger according to the Russian hygienic standards) was 6000 times the MPC, and beryllium (a 1st-class danger) exceeded the MPC a factor of 100. However, arsenic stands out among all constituents. Notably, the

Table 1
Major component composition of the solid tailings (wt. %).

	SiO_2	Al_2O_3	Fe_2O_3	CaO	TiO_2	MgO	MnO	Na_2O	K_2O	P_2O_5	BaO	$S_{sulfide}$	$S_{sulfate}$	CO_2
	Komsomolsk tailings													
mean	49.99	13.93	10.54	7.95	1.19	3.24	0.18	2.41	1.58	0.38	0.05	2.35	–	3.2
min	46.37	12.31	9.05	6.50	0.88	2.60	0.14	1.97	1.11	0.28	0.04	0.64	< 0.1	1.9
max	53.75	15.50	11.64	8.74	1.40	4.40	0.20	2.80	2.05	0.46	0.06	5.59	0.68	4.5
st. dev.	2.06	0.98	0.86	0.73	0.18	0.52	0.02	0.25	0.30	0.06	0.01	1.51	–	0.7
	Berikul tailings[a]													
mean	22.29	6.60	28.03	6.06	0.49	2.36	0.09	0.48	1.22	0.10	0.07	13.64	12.86	0.49
min	16.89	4.17	16.09	4.34	0.367	1.58	0.033	0.47	0.75	0.000	0.034	< 0.1	3.1	0.02
max	36.05	8.42	37.06	9.77	0.73	2.96	0.282	0.49	1.69	0.142	0.33	21.6	20	1.98
st. dev.	5.41	1.28	5.43	1.51	0.097	0.47	0.077	0.008	0.26	0.041	0.092	6.7	5.5	0.60

[a] According to Sidenko et al. (2005) with additions from the present study.

Table 2
Trace element composition of the solid tailings (ppm).

	Cu	Zn	Pb	Cd	Cr	Ni	As	Sb	Te	Se	Sn	Mo	V	Sr	Rb	Ag
	Komsomolsk tailings															
mean	170	780	430	1.9	29	43	1900	830	1.2	0.77	10	1.4	96	330	28	1.5
min	40	110	10	< 0.05	4.0	11	170	200	< 0.01	< 0.01	0.49	0	48	200	18	0.15
max	930	2400	1100	5.0	94	98	5100	2100	2.7	4.3	64	4.2	170	460	38	5.7
st. dev.	190	590	280	1.4	28	21	1500	520	0.81	1.3	17	1.2	33	85	6.3	1.4
	Berikul tailings															
mean	420	1800	560	32	180	52	12000	21	1.6	0.20	1.2	1.7	240	150	14	7.1
min	160	380	120	11	124	27	8600	9.4	0.66	< 0.01	0.75	1.1	180	100	4.3	3.5
max	770	4200	890	67	240	74	18000	35	2.0	0.79	2.1	2.1	310	250	21	9.8
st. dev.	270	1700	330	27	48	21	4300	11	0.63	0.40	0.62	0.45	60	65	7.0	2.7

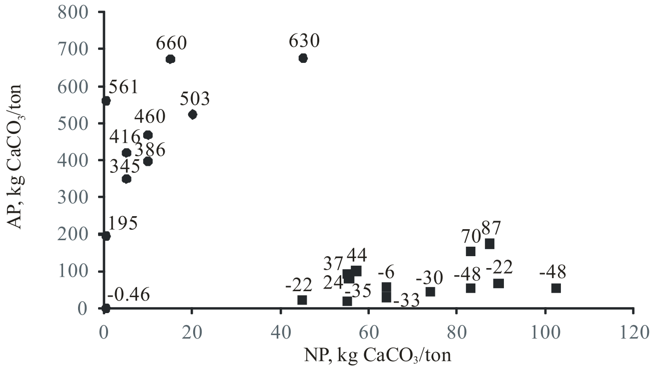

Fig. 2. Calculated acid generation (AP) and acid neutralization (NP) potentials of the Komsomolsk (black squares) and Berikul tailings (black points). Numbers under points indicate NAP values.

average As content is five orders of magnitude higher than the MPC, and the maximum level is six orders higher than the MPC.

The element percentages in the weight equivalent of 1 kg of solids and 1 L of co-existing solution in the solid-water system were calculated. The comparative results for the two described systems, i.e., the “Komsomolsk tailings – tailings pond” and “Berikul tailings – acid pond”, are shown in Fig. 4S (Supplementary Material). This figure shows that the total concentrations and the mobile (water soluble) species of most elements, especially metals (e.g., Fe, Cu, Zn, Ni, and Cd) and metalloids (e.g., As and Sb), are significantly higher in the Berikul tailings than in the Komsomolsk tailings.

Under the prevailing pH/Eh regime, hydrated cations are the predominant species of soluble Na (99%), K (99%), Ca (75%), and Mg (71%) in the Komsomolsk pond, with a significant proportion of $MeHPO_{4(aq)}$ associated with Ca (11%) and Mg (14%). Hydroxide complexes are the predominant species for Al, Fe, Cu, and Pb. According to the dissociation constants of arsenic acid, $HAsO_4^{2-}$ predominates with a small proportion of $H_2AsO_4^-$. The predominant species of soluble Sb (V) is SbO_3^-. Other heavy metals, such as Ni, Zn Cd, and Mn, generally presented as hydrated cations, and hydroxide complexes were the predominant species for Cu and Pb (Fig. 5S (a) in Supplementary Material). Although the sulfate concentration in sample k-5 was 230 mg L^{-1}, sulfate species levels did not reach 13% for the metals (pH 8.2).

The identification of supersaturated solutions can be used as a tool for geo-ecologists to manage the water in the tailings impoundment. The calculations confirmed that the Komsomolsk tailings impoundment water is supersaturated with respect to calcite, dolomite, quartz, barite and apatite. The trace element composition of apatite could be very diverse; therefore, supersaturation with respect to heavy metal phosphates could mean that they were incorporated in apatite (Fig. 6S (b) in Supplementary Material). This issue is also applicable for iron (hydr) oxides, such as ferrihydrite, goethite, etc., that can incorporate all heavy metals (Gadde and Laitinen, 1974; Komárek et al., 2013). Moreover, iron (hydr)oxides can incorporate up to 4% of Sb (V) and 1% of As (V), as revealed by previous scanning electron microscopy (Bortnikova et al., 2006). In addition, the hydroxide sulfate minerals of Cu, Pb, and Zn (Fig. 6S (b) in Supplementary Material) were mainly found in drained tailings sand near the shore.

In the Berikul pond water, which has a pH of 2.15 (sample b-1), hydrated cations are the predominant species of K^+ (86%) and Na^+ (87%), although $MeSO_4^-$ accounts for the remaining 13–14% of species at an SO_4^{2-} concentration of 40,000 mg L^{-1}. For soluble Ca and Mg, the predominant species is $MeSO_{4(aq)}$, and for soluble Al and Fe, the predominant species are $Me(SO_4)_2^-$ and $MeSO_4^+$, with a small proportion of Me^{3+}. According to the stability constants of heavy metals

Table 3
Composition of the Komsomolsk tailings pond water, where SO_4^{2-}-Sb is in mg L^{-1} and Al-Ti is in µg L^{-1} (according to RMH, 2003).

	k-1	k-2	k-3	k-4	k-5	k-6	k-7	k-8	k-9	MPC_{dw}
pH	7.39	8.09	8.07	8.08	8.23	8.18	8.19	8.14	8.1	
Eh	490	450	420	390	360	440	370	410	370	
EC, µS/cm	574	480	610	620	584	630	590	618	526	
SO_4^{2-}	240	202	310	290	230	290	270	270	220	500
HCO_3^-	24	12	32	18	54	79	24	26	16	
Cl^-	2.0	6.0	5.4	7.1	6.3	8.5	8.9	4.2	2.5	350
F^-	1.2	1.3	1.8	1.9	1.6	1.5	3.8	3.2	2.5	
NO_3^-	14	12	8.5	15	6.3	23	5.4	12	9.2	45
Ca^{2+}	91	83	86	80	87	81	90	86	87	
Mg^{2+}	16	16	16	17	17	18	18	17	17	50
Na^+	13	17	16	17	18	20	19	19	17	200
K^+	3.9	3.0	3.0	2.9	2.9	3.1	3.2	3.0	3.2	
Si	2.1	1.5	1.4	1.4	1.3	1.2	1.1	1.0	1.3	10
Fe	0.47	0.39	0.33	0.34	0.36	0.33	0.42	0.39	0.084	0.3
As	0.12	0.22	0.21	0.22	0.22	0.22	0.23	0.22	0.18	0.01
Sb	0.26	0.89	0.89	0.86	0.90	0.91	0.93	0.90	0.54	0.005
Al	10	44	51	33	46	39	81	36	74	200
Mn	8	28	16	17	26	25	24	24	14	100
Cu	3.9	4.4	3.6	1.9	2.5	2.5	3.0	1.9	4.2	1000
Zn	4.1	23	11	18	18	32	239	31	7	1000
Pb	1.2	0.93	1.0	0.9	1.3	1.1	1.4	1.3	1.1	10
Cd	0.15	3.7	18	0.60	0.7	1.3	1.7	0.15	0.12	1
Ba	27	52	52	51	56	61	66	52	65	700
Sr	240	316	306	296	315	317	321	301	340	7000
Cr	2.7	1.0	0.75	1.8	0.38	0.23	0.8	1.2	2.2	50
Co	0.49	0.37	0.33	0.35	0.40	0.33	0.50	0.37	0.44	100
Ni	3.2	1.0	1.3	0.24	0.77	0.91	0.47	0.13	2.6	20
V	0.42	0.35	1	0.37	0.41	0.29	< 0.1	0.40	0.54	100
P	31	51	44	11	48	52	196	59	16	
Ti	5.8	6.3	5.1	5.1	4.8	4.8	5.9	4.7	4.6	100

with sulfate ions (Ball and Nordstrom, 1991), the proportion of the associated sulfate complexes increases in the following order: Pb > Cd > Zn > Ni, Cu > Mn. Aqueous species of As in the solutions are not limited to arsenic acid. Specifically, iron-arsenate species $FeHAsO_4^+$ (18%) and $FeH_2AsO_4^{2+}$ (14%) can form because the total concentration of iron in the acidic solution is 5500 mg L^{-1} (Table 4).

The calculations confirmed that the Berikul pond water is supersaturated with respect to sulfate minerals, quartz and goethite (Fig. 6S (b) in Supplementary Material). This is typical acid sulfate supergene alteration assemblage that includes jarosite, barite, gypsum and anglesite. Acid solutions are undersaturated with respect to many of the soluble minerals, such as $MeSO_4{\cdot}nH_2O$, where Me represents divalent

Table 4
Chemical composition of the Berikul ponds water (mg L^{-1}).

Parameter	b-1	b-2	b-3	b-4	b-5	b-6	b-7	b-8
pH	2.15	2.23	2.23	2.25	1.79	2.13	2.46	2.25
EC, µS/cm	9500	5900	7600	5900	16300	6460	3330	11000
SO_4^{2-}	40000	18400	30000	15000	76000	17000	8400	37000
Ca^{2+}	280	420	270	300	500	360	210	530
Mg^{2+}	240	110	220	91	680	120	60	620
Na^+	12	8.3	4.1	5.3	27	2.6	1.5	3.7
K^+	0.66	0.44	0.07	0.50	0.76	0.54	0.12	0.62
Si	41	40	30	38	69	25	14	66
Fe	5400	2100	3600	1400	20000	2700	670	7200
As	1300	340	810	110	4100	450	59	290
Sb	3.8	1.6	2.5	1.0	4.1	1.2	1.1	2.1
Al	350	150	360	170	1200	210	110	800
Mn	13	8.3	14	5.8	36	8.3	6.5	75
Cu	22	11	23	8.4	69	12	4.3	19
Zn	130	54	79	46	370	63	24	210
Pb	13	2.8	5.3	1.3	29	2.4	< 0.03	3.1
Cd	3.3	1.2	2.0	1.1	10	1.7	0.6	3.9
Ba	0.11	0.19	0.052	0.069	0.019	0.02	0.015	0.009
Sr	0.81	0.87	0.46	0.65	1.1	0.33	0.20	0.44
Cr	2.6	0.79	1.99	1.1	7.6	0.80	0.16	1.3
Co	2.7	1.1	2.5	0.88	8.9	1.5	0.63	4.9
Ni	4.9	2.1	4.4	1.7	16	2.6	0.98	11
V	0.85	0.33	0.50	0.32	3.8	0.73	0.20	1.4
P	19	6.4	15	1.9	40	5.3	0.81	4.6
Ti	6.2	1.5	2.6	0.90	22	1.9	0.24	0.52
Li	0.28	0.14	0.24	0.14	0.85	0.20	0.12	0.53
Be	0.008	0.0045	0.011	0.0058	0.021	0.002	0.003	0.02

Fe, Ni, Cu, Zn, Cd and Mn. Although jarosite plays an important role because of its ability to remove metals from solution during precipitation, it becomes increasingly unstable with increasing pH and transforms into ferrihydrite and goethite (Murray et al., 2014).

It is important to consider examples of particular reactions of mineral precipitation. Considering these reactions is particularly important for the Berikul tailings due to the rich variety of secondary minerals present ($S_{sulfate}$ content up to 20%). These minerals include melanterite, solid solutions of jarosite $(H_3O,K,Na)Fe_3^{3+}(SO_4)_2(OH)_6$, iron-sulfur arsenates, sarmientite $Fe_2^{3+}(AsO_4)(SO_4)OH \times 5H_2O$ and two amorphous phases of Fe and As (Gieré et al., 2003). For example, the reactions of natural and synthetic melanterites with water lead to a rapid (2–3 min after addition to water) decrease in pH values from neutral to 2.8 according to laboratory experiments (Frau, 2000). Melanterite dissolution releases ferrous ions, which are oxidized to ferric ions, and the hydrolysis leads to the release of protons.

$$FeSO_4{\cdot}7H_2O_{(s)} \leftrightarrow Fe^{2+} + SO_4{}^{2-} + 7H_2O \tag{4}$$

$$4Fe^{2+} + 4H^+ + O_{2(g)} \rightarrow 4Fe^{3+} + 2H_2O \tag{5}$$

$$Fe^{3+}{}_{(aq)} + 3H_2\ O\rightarrow Fe(OH)_3 + 3H^+ \tag{6}$$

$$FeSO_4{\cdot}7H_2O_{(s)} + 0.25O_{2(g)} \rightarrow Fe(OH)_{3(s)} + SO_4{}^{2-} + 2H^+ + 4.5H_2O \tag{7}$$

$$KFe_3(SO_4)_2(OH)_{6(s)} + 3H_2\ O\Rightarrow 3Fe(OH)_{3(s)} + 2SO_4{}^{2-} + 3H^+ + K^+\ (pH > 4) \tag{8}$$

$$KFe_3(SO_4)_2(OH)_{6(s)} + 6H^+ \Rightarrow 3Fe^{3+} + 2SO_4{}^{2-} + K^+ + 6H_2O\ (pH < 3) \tag{9}$$

$$KFe_3(SO_4)_2(OH)_{6(s)} + 4H_2\ O\Rightarrow 3[Fe(OH)_2{\cdot}4(H_2O)]^+ + 2SO_4{}^{2-} + K^+\ (3 < pH < 4) \tag{10}$$

Thus, acidic solutions are produced during the interactions involving seasonal precipitation and the Berikul tailings. However, jarosite is slightly soluble, and the specifics of the reactions are as follows. At a pH greater than 4, ferric hydroxide is precipitated, and hydrogen cations are emitted (8). At a pH less than 4, jarosite dissolution occurs with the consumption of hydrogen cations (9), and at pH values from 3 to 4, dissolution occurs without the release or consumption of protons (10).

Because of its relatively low solubility, the amount of acid contributed by jarosite dissolution is small relative to that produced from the dissolution of more soluble iron sulfates. Gault et al. (2005) proved that jarosites (and hydrous ferric oxides) are effective scavengers of arsenic. However, increasing the moisture content can lead to jarosite dissolution and the concomitant release of arsenic impurities (Elwood Madden et al., 2012; Smith et al., 2006; Welch et al., 2008).

The unsuspected surface drainage stream, which flows into the Voskresenka River, has a negative impact on the river water quality (Table 5). Before the confluence of the drainage stream (samples v-1 and v-2), elevated concentrations of Fe and Al were found compared to the regional background (Shvartsev et al., 1997; Savichev, 2014). After the drainage stream, the river water is characterized by high contents of As and Sb (samples v-3 – v-5). In drinking water, the arsenic content is 10 times higher than the MPC, as measured in a tubular well (sample kom-8/15) located downhill from the ravine under the tailings dam. In another well (sample kom-7/15), an elevated concentration of arsenic approaching the MPC value was also observed (Fig. 1S in Supplementary Material and Table 5).

The studied ponds that formed on the Berikul mine tailings have acidic and extra-mineralized solutions (up to 100 g L^{-1}) with extremely high As concentrations for any type of water worldwide influenced by the mining industry (Fig. 3). As shown in Fig. 3, As is commonly found in water affected by mine tailings around the world. The elevated As concentrations detected in the drinking water emphasize the need for urgent examination of the old tailings dam to identify the migration pathways into underground horizons.

The surface water chemistry, solid precipitate composition, acid-base relation, and definition of unsatisfactory drinking water quality in local wells were considered in characterizing the Komsomolsk tailings area as a dangerous environmental zone currently and potentially in the future. Additionally, an ERT investigation was conducted to determine the subsurface structure.

4.3. Geophysical investigations

The resistivity section along profile No. 6 and its interpretation are shown in Fig. 7S (Supplementary Material).

A water layer at a certain depth (1.6 m) and the mean electrical conductivity (EC, 550 μS/cm) were used in the model when solving the inverse problem. The mean EC was converted to resistivity (Ω), which was equal to 18 Ω m. From the interpretation of the geoelectric section, the thickness of the tailings in the deepest part of profile No. 6 is 7.5 m based on a resistivity of 25–30 Ω m, and the tailings thickness decreases to 4.5 m in the southeastern area of the tailings pile. The base of the tailings is characterized by diorites with high (1000–3000 Ω m and higher) resistivity. A thin (≈1–1.5 m) weathering crust on diorites can be observed in the upper boundary, where the resistivity decreases to 500 Ω m. In the profile range of 60–80 m to a depth of 15 m, an area of low (80–100 Ω m) resistivity was identified and interpreted as a tailings-filled ravine.

The resistivity of the tailings in the upper part of the section is 25–30 Ω m and increases with depth. According to the data from the KGEP, 79% of the fraction has a mesh size of 200 (less than 0.076 mm), and 18% of the tailings material is in the range of 0.25–0.1 mm. Under the classification of V.V. Okhotin (Dauetas et al., 1993), the material corresponds to a silty loam. According to the relationship between the resistivity of rocks and the mineralization of groundwater (GR, 2004), groundwater with a mineral content equal to 0.5 g L^{-1} corresponds to a sandy loam with a resistance of 25–30 Ω m.

Based on the data interpretation, the thickness of the tailings for all obtained ERT profiles was determined, and a thickness map of the tailings was constructed (Fig. 7S in Supplementary Material). The tailings thickness varies from a few meters at the periphery of the tailings to 26 m in deep localized areas near the upper boundary of the bedrock. The median thickness is 7.6 m. The presence of a tailings area of abnormal thickness was confirmed by the increase in the dam height to 25–28 m at a sharp subsiding surface (see satellite image in Fig. 8S in Supplementary Material).

Using the *Volume* tool in Surfer (Golden Software), the tailings volume was calculated as 958,000 m^3. The average density of the tailings is 3.2 g/cm^3; consequently, the weight of the accumulated tailings is ≈ 3 million tons. Thus, it is possible to estimate the quantities of toxic and valuable components within the tailings. For instance, the silver content in the tailings is 1.5 g per ton. Consequently, the general forecasted silver resources are estimated at 4.5 tons. The average arsenic content is 1900 g/t (Table 2); hence, the total amount of arsenic is equal to 5700 tons.

The 3D model of the resistivity distribution based on the results of the three-dimensional inversion of the ERT data is shown in Fig. 9S (Supplementary Material). Bedrock with resistivity values of 500–3000 Ω m is colored red in the 3D model. Tailings with resistivity values less than 100 Ω m are highlighted as semitransparent areas. The resistivity isosurface, which is equal to 200 Ω m, emphasizes the bottom topography of the tailings dump, including local depressions, as previously identified in Fig. 8S (Supplementary Material).

The equal resistivity line maps at depths of 4 and 20 m, which are sections of the 3D model, are shown in Fig. 4. The resistivity distribution at a depth of 4 m and the minimum tailings resistivity values are 40–60 Ω m, which reflects a relatively low-salinity pore water (250–300 mg L^{-1}). However, a local anomaly of low (20–30 Ω m) resistivity associated with an increase in the mineralization of pore water

Table 5
Composition of the water in the Voskresenka River and the drinking water of the Komsomolsk settlement (mg L^{-1}).

Parameter	The Voskresenka River					drinking water from water-pump				
	before drainage stream			after drainage stream		40 m	25 m	20 m	25 m	18 m
	v-1	v-2	v-3	v-4	v-5	kom-7/15	kom-8/15	kom-9/15	kom-10/15	kom-12/15
pH	7.2	7.32	7.53	7.57	7.70	7.60	7.51	7.48	7.38	7.46
Eh, mV	487	474	475	466	457	240	467	478	497	462
EC, μS/cm	330	323	363	364	377	592	381	350	222	624
SO_4^{2-}	33	29	33	43	54	23	28	7.1	12	49
Cl^-	23	19	19	16	12	12	13	0.40	4.5	32
Ca	60	59	64	65	67	79	66	75	36	81
Mg	5.7	5.8	7.2	7.6	8.1	7.3	10	2.8	5.9	24
Na	4.6	4.6	5.6	5.7	6.5	3.7	3.9	2.3	4.6	11
K	0.91	0.91	1.1	1.0	1.2	1.5	1.4	0.23	0.34	3.4
Si	5.2	5.5	5.3	5.6	4.7	4.3	7.7	4.9	8.2	7.5
Fe	**0.55**	**0.58**	**0.58**	**0.59**	**0.56**	**0.62**	**0.31**	**0.83**	0.20	**0.46**
Al	**0.37**	**0.41**	**0.33**	**0.33**	**0.28**	< 0.002	0.0047	**0.43**	< 0.002	0.0060
Mn	0.0047	0.0085	**0.027**	**0.026**	**0.034**	0.0015	< 0.0002	0.0076	0.0070	0.00040
As	< 0.002	< 0.002	0.0060	***0.0081***	***0.0084***	***0.0083***	**0.089**	< 0.002	< 0.002	< 0.002
Sb	0.00015	0.00023	0.00048	0.00057	**0.0058**	0.00025	0.00028	< 0.0001	< 0.0001	0.00011
Cu	< 0.002	0.0028	< 0.002	< 0.002	< 0.002	< 0.002	< 0.002	0.0079	< 0.002	< 0.002
Zn	0.0024	0.0043	0.0038	0.0033	0.0036	0.0020	0.0031	0.0061	0.022	< 0.002
Pb	0.0013	0.0017	0.0014	0.0015	0.0014	< 0.0002	0.00075	0.0028	0.00039	0.0007
Ba	0.028	0.025	0.026	0.026	0.025	0.025	0.0034	0.011	0.0029	0.0069

Note: 40 m, 25 m, etc. denote the well depths; bold font indicates a concentration exceeding the MPC; and bold italic font indicates a concentration approaching the MPC.

to 500–750 mg L^{-1} can be observed at a depth of 20 m.

This anomalous area is likely associated with the infiltration of acid solutions into deep horizons from the area of the Berikul mine tailings, in which the TDS concentration in the ponds reaches more than 100 g L^{-1}. According to the resistivity distribution at a depth of 20 m, the infiltration path of contaminated waters can be traced. Groundwater contaminated by AMD flows from the tailings dump to the discharge area, which is located under the dam, and then along the fault until the acid solutions reach the drinking water horizons (20–40 m depth). The arrow shows the estimated path of contaminated water movement. Groundwater contamination was confirmed via an analysis of drinking water from a well (sample No. d-8, Table 5) located near the fault.

To identify the localized leakage path from the tailings dump, the geoelectric section across the dam was analyzed (Fig. 5). The base of the section is diorite with high resistivity, varying from 500 to 3000 Ω m, depending on the fracture. At a distance of 100–155 m in the profile and at a depth of 8 m, a notable anomaly of low (3.5–7.5 Ω m) resistivity can be identified. This anomaly corresponds to mineralization at a rate of 15–20 g L^{-1}.

These geophysical data should be used to develop an antifiltering screen in the body of the dam to prevent further groundwater contamination. The study demonstrates that the former mining activities are responsible for the high As concentrations in the water bodies (surface water and groundwater). Based on the geochemical and geophysical measurements, it is evident that drainage from the BGEP

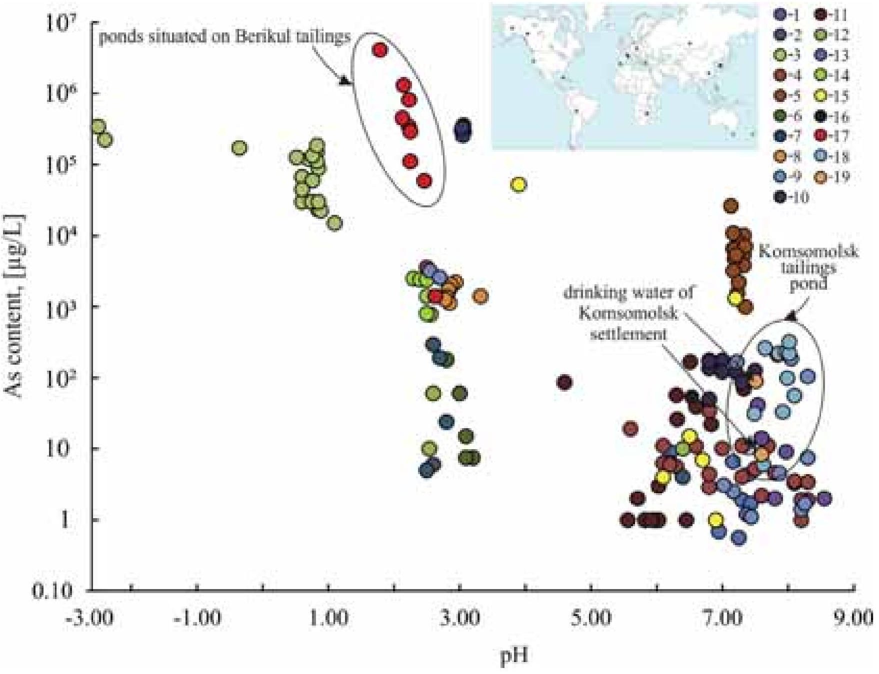

Fig. 3. Arsenic content in ground and surface waters in areas affected by mine tailings: 1- Cerro Rico AMD, Bolivia (Strosnider et al., 2011); 2- Santa Lucia mine, Cuba (Romero et al., 2010); 3- Richmond mine, USA (Nordstrom et al., 2000; Druschel et al., 2004); 4- Kantishna Hills, Alaska, USA (Ritchie et al., 2013); 5- Zloty Stok mining area, Poland (Marszałek and Wąsik, 2000); 6- Enguiales mine, France (Courtin-Nomade et al., 2005); 7- Carnoules mine, France (Casiot et al., 2003); 8- Iberian pyritic belt, SW Spain (Asta et al., 2010); 9- Alaşehir Hg mine, Turkey (Gemici, 2008); 10- Beatrice gold mine, Zimbabwe (Ravengai et al., 2005); 11- Gubong mine, Korea (Woo and Choi, 2001); 12- Ilgwang mine, Busan, Korea (Nguyen et al., 2015); 13- Xikuangshan mining area, China (Fu et al., 2016); 14- Mount Bischoff, Tasmania, Australia (Gault et al., 2005); 15- Blackwater mine, New Zealand (Haffert and Craw, 2008); 16- The Ketza River mine, Canada (Development Assessment Branch, 2005); 17- Ponds situated on the Berikul tailings; 18- Komsomolsk tailings pond; 19- Drinking water of the Komsomolsk settlement. (For interpretation of the references to color in this figure legend, the reader is referred to the Web version of this article.)

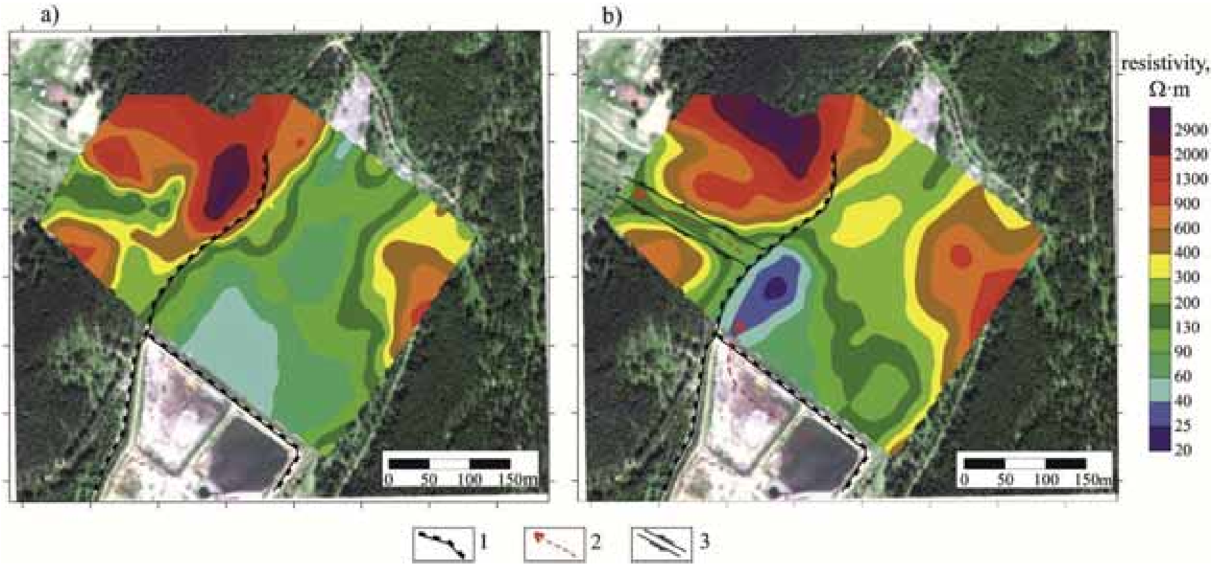

Fig. 4. Maps of the electrical resistivity distribution at depths of 4 m (a) and 20 m (b): 1 – dam; 2 – the hypothetical path of contaminated water infiltration; 3 – fault zone boundaries.

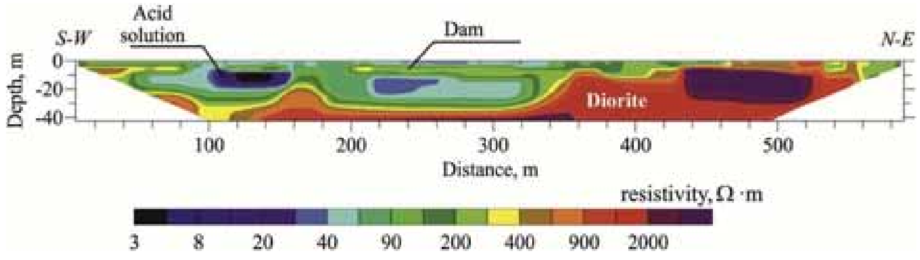

Fig. 5. The geoelectric section through the Komsomolsk tailings dam.

tailings and water from tailing pond (KGEP) are the principal sources of toxic elements. The NAP calculation is reasonable and useful, but it does not always consider the specificity of elements, e.g., sulfate salts are an unconsidered source of toxic substances. These sulfates (7, 8) can dissolve in neutral solutions. Specifically, the Berikul tailings NAP is 415 kg $CaCO_3$/ton and can result in the production of acid leachates in the short and long terms. In addition, the significant contribution of secondary water-soluble minerals to the formation of acid sulfate-arsenate solutions was shown. For the KGEP tailings, NP ~ AP, but the formation of waters containing toxic elements in the future was predicted based on arsenic and antimony concentrations in the solid matter and the continuous leaching of these elements (Fig. 4S in Supplementary Material). Tailings dumps (tailings impoundments) that contain hydrometallurgy wastes (in this case 3.5 million tons of waste) are dangerous because unregulated storage often leads to the erosion of the enclosing dams or the use of ponds by the local population for domestic purposes.

4.4. Economic evaluation of the environmental damage

As noted above, the numerical value of the damage $\gamma_{\text{в}}$ to water resources located in the Kemerovo region was determined according to the cited methodology (Girusov et al., 2003). In 1999, the damage was estimated at 180 USD per ton of materials. The recent value cited by GR (1999) was used to assess the damage in 2017. Thus, considering the dynamics of inflation for the period of 1999–2017, the damage to water resources is 997 USD per ton.

In calculating the economic damage, a coefficient of environmental significance of $\sigma_{\text{в}} = 0.92$ for water bodies in the Kemerovo region was applied. Indicators of relative danger A_i were calculated based on the hygienic standards (RMH, 2003).

The economic assessment of environmental damage from the Komsomolsk impoundment showed that the annual damage caused by drainage pollution to the Voskresenka River is 912,000 USD and that the annual damage caused by groundwater pollution is 597,000 USD.

The geophysical investigation and economic evaluation can be used to develop a remediation scheme and estimate costs regarding the extraction of valuable components.

5. Conclusions

1 The results of the study showed that AP and NP are both equal to 73 kg $CaCO_3$/t for the Komsomolsk tailings and that AP and NP are equal to 426 and 11 kg $CaCO_3$/t for the Berikul tailings, respectively. Most of the analyzed element (Fe, Pb, Cd, Cu, Zn, Se, As, Sb, etc.) concentrations in the Komsomolsk tailings pond (pH ~8) do not exceed the MPC values. The two exceptions are arsenic and antimony, which exceed the MPC by factors of 21 and 170 on average, respectively. Open ponds on the Berikul tailings are sulfate-arsenate-iron-aluminum-type solutions. The element concentrations in the Berikul ponds are much higher than the MPCs of Fe, Al, Mn, Cu, Zn, Cd, Co, Ni, As, and, Sb. These acid (pH 2) and extra-mineralized solutions (up to 100 g L^{-1}) have the highest As concentrations ever reported.

2 The geophysical investigation (namely, ERT) was the basis for calculating the thickness of the Komsomolsk tailings deposit (approximately 7.6 m) and the tailings volume (958,000 m^3). The infiltration of highly mineralized solutions from the Berikul tailings ponds into the drinking water horizons was traced based on the resistivity distribution at a depth of 20 m along a natural fault. Using

both geophysical and geochemical data, an economic evaluation was conducted. The environmental damage caused by the pollution of the Voskresenka River and groundwater totaled more than 1.5 million USD per year.

3 The obtained results can be used to determine the redistribution of toxic elements from the technogenic system into the environment, to evaluate potential risks and to design a remediation strategy. The recommended sequence is as follows: 1) an impermeable screen should be installed to prevent drainage leakage from the Komsomolsk tailings under northwest side of the dam; 2) the toxic and valuable components should be extracted from the Berikul solid tailings, and the area should be dewatered; and 3) an impervious barrier should be constructed on the south side of the impoundment, and the residual Berikul tailings should be buried.

Acknowledgments

We wish to thank M. Kirillov, A. Shevko, and D. Kucher for their help during field campaigns and S. Nechepurenko, N. Fedunina, and Yu. Kolmogorov for help with the chemical analyses. This study was financially supported by the Russian Foundation for Basic Research (No. 17-05-00056 and mol_a_dk 16-35-60053) and the Research Project (No. IX.138.3.1) of the Trofimuk Institute of Petroleum Geology and Geophysics SB RAS. The authors thank Prof. Michael Kersten and two anonymous reviewers for their comments on this manuscript. Additionally, the authors are thankful to "American Journal Expert", in particular Dr. Aimee Talarski for editing the manuscript.

Appendix A. Supplementary data

Supplementary data related to this article can be found at http://dx.doi.org/10.1016/j.apgeochem.2018.04.009.

References

Abrosimova, N., Bortnikova, S., Gas'kova, O., Yurkevich, N., Ribkina, E., 2015a. Results of mine tailings – water interaction: a column leaching study on the example of waste materials of Komsomolsky Gold Processing Plant. In: International Multidisciplinary Scientific GeoConference Surveying Geology and Mining Ecology Management, Albena, Bulgaria, 18–24 Jun 2015, Available at: https://sgemworld.at/sgemlib/spip.php?article6354.

Abrosimova, N., Gaskova, O., Loshkareva, A., Edelev, A., Bortnikova, S., 2015b. Assessment of the acid mine drainage potential of waste rocks at the Ak-Sug porphyry Cu-Mo deposit. J. Geochem. Explor. 157, 1–14. https://dx.http://dx.doi.org/10.1016/j.gexplo.2015.05.009.

Alabin, L.V., Kalinin, Yu.A., 1999. Gold Metallogeny of Kuznetsk Alatau. Publishing House, United Institute of Geology, Geophysics, and Mineralogy, Siberian Branch, Russian Academy of Sciences, Novosibirsk, pp. 234.

Armienta, M.A., Villaseñor, G., Cruz, O., Ceniceros, N., Aguayo, A., Morton, O., 2012. Geochemical processes and mobilization of toxic metals and metalloids in an As-rich base metal waste pile in Zimapán. Central Mexico. Appl. Geochem. 27, 2225–2237. https://dx.http://dx.doi.org/10.1016/j.apgeochem.2012.01.015.

Asta, M.P., Ayora, C., Román-Ross, G., Cama, J., Acero, P., Gault, A.G., Charnock, J.M., Bardelli, F., 2010. Natural attenuation of arsenic in the Tinto Santa Rosa acid stream (Iberian Pyritic Belt, SW Spain): the role of iron precipitates. Chem. Geol. 271, 1–12. https://dx.http://dx.doi.org/10.1016/j.chemgeo.2009.12.005.

Bailey, B.L., Blowes, D.W., Smith, L., Sego, D.C., 2015. The Diavik Waste Rock Project: geochemical and microbiological characterization of drainage from low-sulfide waste rock: active zone field experiments. Appl. Geochem. 62, 18–34. https://dx.http://dx.doi.org/10.1016/j.apgeochem.2015.02.014.

Balci, N., Demirel, C., 2018. Prediction of acid mine drainage (AMD) and metal release sources at the Küre Copper Mine Site, Kastamonu, NW Turkey. Mine Water Environ. 37 (1), 56–74. https://doi.org/10.1007/s10230-017-0470-4.

Balkov, E.V., Panin, G.L., Manshtein, Y.A., Manshtein, A.K., Beloborodov, V.A., 2012. Electrotomography: equipment, technique, and application. Geophysics 6, 54–63.

Ball, J.W., Nordstrom, D.K., 1991. User's Manual for WATEQ4F, with Revised Thermody Namic Data Base and Test Cases for Calculating Speciation of Major, Trace, and Redox Elements in Natural Waters: United States Geological Survey Open-file Report 91-183. United States Geological Survey, Menlo Park, California.

Baryshev, V.A., Kolmogorov, Y.P., Kulipanov, G.N., Scrinsky, A.N., 1986. X-ray fluorescent method with synchrotron radiation. J. Anal. Chem. 41, 389–401. https://dx.http://dx.doi.org/10.1016/0168-9002(86.

Blowes, D.W., Jambor, J.L., Hanton-Fong, C.J., Lortie, L., Gould, W.D., 1998. Geochemical, mineralogical and microbiological characterization of a sulphide-bearing carbonate-rich gold-mine tailings impoundment, Joutel, Québec. Appl. Geochem. 13, 687–705. https://dx.http://dx.doi.org/10.1016/S0883-2927(98.

Blowes, D.W., Ptacek, C.J., Jambor, J.L., Weisener, C.G., Paktunc, D., Gould, W.D., Johnson, D.B., 2014. The Geochemistry of Acid Mine Drainage. Treatise on Geochemistry, second ed. Elsevier, Oxford, pp. 131–190. https://doi.org/10.1016/B978-0-08-095975-7.00905-0.

Bobachev, A.A., Gorbunov, A.A., 2005. Two-dimensional electric resistivity and induced polarization survey: equipment, technique, and software. Razvedka Ohrana Nedr. 12, 52–54.

Bodénan, F., Baranger, P., Piantone, P., Lassin, A., Azaroual, M., Gaucher, E., Braibant, G., 2004. Arsenic behaviour in gold-ore mill tailings, Massif Central, France: hydrogeochemical study and investigation of in situ redox signatures. Appl. Geochem. 19, 1785–1800. https://dx.http://dx.doi.org/10.1016/j.apgeochem.2004.03.012.

Bortnikova, S., Gaskova, O., Airiyants, A., 2003. Technogenic Lakes Substance Accumulation, Evolution, and Influence on the Environment. Academic publishing house "Geo", Novosibirsk.

Bortnikova, S., Gaskova, O., Bessonova, E., 2006. Geochemistry of Technogenic System. Academic publishing house "Geo", Novosibirsk.

Bortnikova, S.B., Gas'kova, O.L., Prisekina, N.A., 2010. Geochemical estimation of the potential danger of waste rocks from the Veduginskoe deposit. Geochem. Int. 48, 280–294. https://dx.http://dx.doi.org/10.1134/S0016702910030055.

Bortnikova, S., Bessonova, E., Gaskova, O., 2012. Geochemistry of arsenic and metals in stored tailings of a Co-Ni arsenide-ore, Khovu-Aksy area, Russia. Appl. Geochem. 27, 2238–2250. https://dx.http://dx.doi.org/10.1016/j.apgeochem.2012.02.033.

Bowell, R.J., Bruce, I., 1995. Geochemistry of iron ochres and mine waters from Levant Mine. Cornwall. Appl. Geochem. 10, 237–250. https://dx.http://dx.doi.org/10.1016/0883-2927(94.

Casiot, C., Morin, G., Juillot, F., Bruneel, O., Personné, J.-C., Leblanc, M., Duquesne, K., Bonnefoy, V., Elbaz-Poulichet, F., 2003. Bacterial immobilization and oxidation of arsenic in acid mine drainage (Carnoulès creek, France). Water Res. 37, 2929–2936. https://dx.http://dx.doi.org/10.1016/S0043-1354(03.

Çelebi, E.E., Öncel, M.S., 2016. Determination of acid forming potential of massive sulfide minerals and the tailings situated in lead/zinc mining district of Balya (NW Turkey). J. African Earth Sci. 124, 487–496. https://dx.http://dx.doi.org/10.1016/j.jafrearsci.2016.09.014.

Cheng, Y.-Y., Huang, N.-C., Chang, Y.-T., Sung, J.-M., Shen, K.-H., Tsai, C.-C., Guo, H.-R., 2017. Associations between arsenic in drinking water and the progression of chronic kidney disease: a nationwide study in Taiwan. J. Hazard Mater. 321, 432–439. https://dx.http://dx.doi.org/10.1016/j.jhazmat.2016.09.032.

Choong, T.S.Y., Chuah, T.G., Robiah, Y., Gregory Koay, F.L., Azni, I., 2007. Arsenic toxicity, health hazards and removal techniques from water: an overview. Desalination 217, 139–166. https://dx.http://dx.doi.org/10.1016/j.desal.2007.01.015.

Cidu, R., Biddau, R., Dore, E., Vacca, A., Marini, L., 2014. Antimony in the soil-water-plant system at the Su Suergiu abandoned mine (Sardinia, Italy): strategies to mitigate contamination. Sci. Total Environ. 497–498, 319–331. https://dx.http://dx.doi.org/10.1016/j.scitotenv.2014.07.117.

Cidu, R., Da Pelo, S., Frau, F., 2013. Legacy of cyanide and ARD at a low-scale gold mine (Furtei, Italy). Mine Water Environ. 32 (2), 74–83. https://dx.http://dx.doi.org/10.1007/s10230-012-0209-1.

Courtin-Nomade, A., Bril, H., Neel, C., Lenain, J.-F., 2003. Arsenic in iron cements developed within tailings of a former metalliferous mine-Enguialès, Aveyron, France. Appl. Geochem. 18, 395–408. https://dx.http://dx.doi.org/10.1016/S0883-2927(02.

Courtin-Nomade, A., Grosbois, C., Bril, H., Roussel, C., 2005. Spatial variability of arsenic in some iron-rich deposits generated by acid mine drainage. Appl. Geochem. 20, 383–396. https://dx.http://dx.doi.org/10.1016/j.apgeochem.2004.08.002.

Cravotta, C.A., 2008. Dissolved metals and associated constituents in abandoned coal-mine discharges, Pennsylvania, USA. Part 1: constituent quantities and correlations. Appl. Geochem. 23, 166–202. https://dx.http://dx.doi.org/10.1016/j.apgeochem.2007.10.011.

Cullen, W.R., Reimer, K.J., 1989. Arsenic speciation in the environment. Chem. Rev. 89, 713–764. https://dx.http://dx.doi.org/10.1021/cr00094a002.

Dauetas, A.A., Denisyuk, I.I., Kuzmenko, A.A., Vorobev, V.D., 1993. Seismic Effects of Blasting in Rock. CRC Press.

Development Assessment Branch, 2005. Final Screening Report Ketza River Mine Care and Maintenance Water Licence Application.

Dousova, B., Buzek, F., Rothwell, J., Krejcova, S., Lhotka, M., 2012. Adsorption behavior of arsenic relating to different natural solids: soils, stream sediments and peats. Sci. Total Environ. 433, 456–461.

Drahota, P., Filippi, M., 2009. Secondary arsenic minerals in the environment: a review. Environ. Int. 35, 1243–1255. https://dx.http://dx.doi.org/10.1016/j.envint.2009.07.004.

Druschel, G.K., Baker, B.J., Gihring, T.M., Banfield, J.F., 2004. Acid mine drainage biogeochemistry at Iron Mountain, California. Geochem. Trans. 5, 13–32. https://dx.http://dx.doi.org/10.1186/1467-4866-5-13.

Edraki, M., Golding, S.D., Baublys, K.A., Lawrence, M.G., 2005. Hydrochemistry, mineralogy and sulfur isotope geochemistry of acid mine drainage at the Mt. Morgan mine environment, Queensland, Australia. Appl. Geochem. 20, 789–805. https://dx.http://dx.doi.org/10.1016/j.apgeochem.2004.11.004.

El Adnani, M., Plante, B., Benzaazoua, M., Hakkou, R., Bouzahzah, H., 2016. Tailings weathering and arsenic mobility at the abandoned Zgounder Silver Mine, Morocco. Mine Water Environ. 35, 508–524. https://dx.http://dx.doi.org/10.1007/s10230-015-0370-4.

Elwood Madden, M.E., Madden, A.S., Rimstidt, J.D., Zahrai, S., Kendall, M.R., Miller, M.A., 2012. Jarosite dissolution rates and nanoscale mineralogy. Geochim. Cosmochim. Acta. 91, 306–321. https://dx.http://dx.doi.org/10.1016/j.gca.2012.05.001.

Fan, C.-S., Tseng, S.-C., Li, K.-C., Hou, C.-H., 2016. Electro-removal of arsenic(III) and arsenic(V) from aqueous solutions by capacitive deionization. J. Hazard Mater. 312, 208–215. https://dx.http://dx.doi.org/10.1016/j.jhazmat.2016.03.055.

Foster, A.L., Brown, G.E., Tingle, T.N., Parks, G.A., 1998. Quantitative arsenic speciation in mine tailings using X-ray absorption spectroscopy. Am. Min. 83, 553–568. https://dx.http://dx.doi.org/10.2138/am-1998-5-616.

Frau, F., 2000. The formation-dissolution-precipitation cycle of melanterite at the abandoned pyrite mine of Genna Luas in Sardinia, Italy: environmental implications. Mineral. Mag. 64, 995–1006. https://dx.http://dx.doi.org/10.1180/002646100550001.

Fu, Z., Wu, F., Mo, C., Deng, Q., Meng, W., Giesy, J.P., 2016. Comparison of arsenic and antimony biogeochemical behavior in water, soil and tailings from Xikuangshan, China. Sci. Total Environ. 539, 97–104. https://dx.http://dx.doi.org/10.1016/j.scitotenv.2015.08.146.

Fuller, C.C., Davis, J.A., Waychunas, G.A., 1993. Surface chemistry of ferrihydrite: Part 2. kinetics of arsenate adsorption and coprecipitation. Geochem. Cosmochim. Acta 57, 2271–2282.

Gadde, R.R., Laitinen, H.A., 1974. Heavy metal adsorption by hydrous iron and manganese oxides. Anal. Chem. 46 (13), 2022–2026.

Gas'kova, O.L., Bortnikova, S.B., Airiyants, A.A., Kolmogorov, Y.P., Pashkov, M.V., 2000. Geochemical features of an anthropogenic impoundment with cyanidation wastes of gold-arsenopyrite-quartz ores. Geochem. Int. 38, 281–291.

Gas'kova, O.L., Shironosova, G.P., Bortnikova, S.B., 2008. Thermodynamic estimation of the stability field of bukovskyite, an iron sulfoarsenate. Geochem. Int. 46 (1), 85–91.

Gault, A.G., Cooke, D.R., Townsend, A.T., Charnock, J.M., Polya, D.A., 2005. Mechanisms of arsenic attenuation in acid mine drainage from Mount Bischoff, western Tasmania. Sci. Total Environ. 345, 219–228. https://dx.http://dx.doi.org/10.1016/j.scitotenv.2004.10.030.

Gemici, Ü., 2008. Evaluation of the water quality related to the acid mine drainage of an abandoned mercury mine (Alaşehir, Turkey). Environ. Monit. Assess. 147, 93–106. https://dx.http://dx.doi.org/10.1007/s10661-007-0101-9.

Gieré, R., Sidenko, N., Lazareva, E., 2003. The role of secondary minerals in controlling the migration of arsenic and metals from high-sulfide wastes (Berikul gold mine, Siberia). Appl. Geochem. 18, 1347–1359. https://dx.http://dx.doi.org/10.1016/S0883-2927(03.

Girusov, E.V., Bobylev, S.N., Novoselov, A.L., Chepurny, N.V., 2003. Ecology and Economics of Environmental Management. UNITY-DANA, Edinstvo, Moscow.

GR, 1999. The Procedure for Determining the Prevented Environmental Damage, Approved by the Order of the State Ecology Committee of 30.11. Goscomecologia of Russia, Moscow 1999.

GR, 2004. Engineering Geological Investigations for Construction. Part 6. Rules of Carrying Out Geophysical Investigations SP 11-105-97. Gosstroy Rossii, Moscow.

Haffert, L., Craw, D., 2008. Processes of attenuation of dissolved arsenic downstream from historic gold mine sites. New Zealand. Sci. Total Environ. 405, 286–300. https://dx.http://dx.doi.org/10.1016/j.scitotenv.2008.06.058.

Hiller, E., Tóth, R., Kučerová, G., Jurkovič, Ľ., Šottník, P., Lalinská-Voleková, B., Vozár, J., 2016. Geochemistry of mine tailings from processing of siderite-Cu ores and mobility of selected metals and metalloids evaluated by a pot leaching experiment at the Slovinky Impoundment, Eastern Slovakia. Mine Water Environ. 35, 447–461. https://dx.http://dx.doi.org/10.1007/s10230-016-0388-2.

Kazakis, N., Kantiranis, N., Kalaitzidou, K., Kaprara, E., Mitrakas, M., Frei, R., Vargemezis, G., Tsourlos, P., Zouboulis, A., Filippidis, A., 2017. Origin of hexavalent chromium in groundwater: the example of Sarigkiol Basin. Northern Greece. Sci. Total Environ. 593–594, 552–566. https://dx.http://dx.doi.org/10.1016/j.scitotenv.2017.03.128.

Kefeni, K.K., Msagati, T.A., Mamba, B.B., 2017. Acid mine drainage: prevention, treatment options, and resource recovery: a review. J. Clean. Prod. 151, 475–493.

Kirillov, M.V., Bortnikova, S.B., Gaskova, O.L., 2016. Authigenic gold formation in the cyanidation tailings of gold–arsenopyrite–quartz ore of Komsomolsk deposit (Kuznetski Alatau, Russia). Environ. Earth Sci. 75, 1050. https://dx.http://dx.doi.org/10.1007/s12665-016-5852-6.

Komárek, M., Vaněk, A., Ettler, V., 2013. Chemical stabilization of metals and arsenic in contaminated soils using oxides-a review. Environ. Pollut. 172, 9–22.

Korneeva, T.V., Yurkevich, N.V., Aminov, P.G., 2017. Geochemical features of migration flows in the impact zone of mining technogenesis (Mednogorsk). Bull. Tomsk Polytech. Univ. Geo Assets Eng. 328, 85–94.

Lazareva, E.V., Bortnikova, S.B., Kolmogorov, U.P., Kireev, A.G., Tsimbalist, V.G., 1999. Metal redistribution within the sulfide tailings body. In: Proceedings of the 5th International Symposium on the Geochemistry of the Earth Surface, . https://www.crcpress.com/Geochemistry-of-the-Earths-Surface-Proceedings-of-the-5th-international/Armannsson/p/book/9789058090737.

Loke, M.H., 2000. Electrical Imaging Surveys for Environmental and Engineering Studies, a Practical Guide to 2D and 3D Surveys. (Penang, Malaysia).

Lottermoser, B.G., 2010. Mine Wastes. Characterization, Treatment, Environmental Impacts, second ed. Springer-Verlag, Berlin Heidelberg, pp. 335.

Marszałek, H., Wąsik, M., 2000. Influence of arsenic-bearing gold deposits on water quality in Zloty Stok mining area (SW Poland). Environ. Geol. 39, 888–892. https://dx.http://dx.doi.org/10.1007/s002549900036.

Martín-Crespo, T., Martín-Velázquez, S., Gómez-Ortíz, D., 2010. A geochemical and geophysical characterization of sulfide mine ponds at the Iberian Pyrite Belt (Spain). Water, Air, Soil Pollut. 217, 387–405. https://dx.doi.org/10.1007/s11270-010-0595-6.

Martin-Crespo, T., Gomez-Ortiz, D., Martin-Velazquez, S., Maria Esbri, J., de Ignacio-San Jose, C., Jose Sanchez-Garcia, M., Montoya-Montes, I., Martin-Gonzalez, F., 2015. Abandoned mine tailings in cultural itineraries: don Quixote Route (Spain). Eng. Geol. 197, 82–93. https://dx.doi.org/10.1016/j.enggeo.2015.08.008.

Martínez, J., Rey, J., Hidalgo, M.C., Benavente, J., 2012. Characterizing abandoned mining dams by geophysical (ERI) and geochemical methods: the Linares-La Carolina district (southern Spain). Water, Air, Soil Pollut. 223, 2955–2968. https://doi.org/10.1007/s11270-012-1079-7.

Martínez, J., Hidalgo, M.C., Rey, J., Garrido, J., Kohfahl, C., Benavente, J., Rojas, D., 2016. A multidisciplinary characterization of a tailings pond in the Linares-La Carolina mining district, Spain. J. Geochem. Explor. 162, 62–71. https://doi.org/10.1016/j.gexplo.2015.12.013.

Martínez-Pagán, P., Faz, A., Acosta, J.A., Carmona, D.M., Martínez-Martínez, S., 2011. A multidisciplinary study for mining landscape reclamation. a study case on two tailing ponds in the region of Murcia (SE Spain). Phys. Chem. Earth, Parts A/B/C 36, 1331–1344. https://doi.org/10.1016/j.pce.2011.02.007.

Meck, M., Love, D., Mapani, B., 2006. Zimbabwean mine dumps and their impacts on river water quality – a reconnaissance study. Phys. Chem. Earth, Parts A/B/C 31, 797–803. https://dx.http://dx.doi.org/10.1016/j.pce.2006.08.029.

Mondal, P., Majumder, C.B., Mohanty, B., 2006. Laboratory based approaches for arsenic remediation from contaminated water: recent developments. J. Hazard Mater. 137, 464–479. https://dx.http://dx.doi.org/10.1016/j.jhazmat.2006.02.023.

Murray, J., Kirschbaum, A., Dold, B., Guimaraes, E.M., Miner, E.P., 2014. Jarosite versus soluble iron-sulfate formation and their role in acid mine drainage formation at the pan de Azúcar Mine Tailings (Zn-Pb-Ag), NW Argentina. Mineral 4, 477–502. https://dx.http://dx.doi.org/10.3390/min4020477.

Nguyen, V.K., Tran, T., Han, H.-J., Lee, S.-H., Lee, J.-U., 2015. Possibility of bacterial leaching of antimony, chromium, copper, manganese, nickel, and zinc from contaminated sediment. J. Geochem. Explor. 156, 153–161. https://dx.http://dx.doi.org/10.1016/j.gexplo.2015.05.012.

Nordstrom, D.K., 1977. Thermochemical redox equilibria of ZoBell's solution. Geochem. Cosmochim. Acta 41, 1835–1841. https://dx.http://dx.doi.org/10.1016/0016-7037(77.

Nordstrom, D.K., Alpers, C.N., Ptacek, C.J., Blowes, D.W., 2000. Negative pH and extremely acidic mine waters from Iron Mountain, California. Environ. Sci. Technol. 34 (2), 254–258.

Olenchenko, V.V., Kucher, D.O., Bortnikova, S.B., Gas'kova, O.L., Edelev, A.V., Gora, M.P., 2016. Vertical and lateral spreading of highly mineralized acid drainage solutions (Ur dump, Salair): electrical resistivity tomography and hydrogeochemical data. Russ. Geol. Geophys. 57, 617–628. https://dx.http://dx.doi.org/10.1016/j.rgg.2015.05.014.

Paktunc, A.D., 1999. Mineralogical constraints on the determination of neutralization potential and prediction of acid mine drainage. Environ. Geol. 39 (2), 103–112.

Paktunc, D., Foster, A., Laflamme, G., 2003. Speciation and characterization of arsenic in Ketza River mine tailings using X-ray absorption spectroscopy. Environ. Sci. Technol. 37 (10), 2067–2074. https://http://dx.doi.org/10.1021/es026185m.

Paktunc, D., Foster, A., Heald, S., Laflamme, G., 2004. Speciation and characterization of arsenic in gold ores and cyanidation tailings using X-ray absorption spectroscopy. Geochem. Cosmochim. Acta 68 (5), 969–983. https://http://dx.doi.org/10.1016/j.gca.2003.07.013.

Placencia-Gómez, E., Parviainen, A., Hokkanen, T., Loukola-Ruskeeniemi, K., 2010. Integrated geophysical and geochemical study on AMD generation at the Haveri Au-Cu mine tailings, SW Finland. Environ. Earth Sci. 61, 1435–1447. https://doi.org/10.1007/s12665-010-0459-9.

Quansah, R., Armah, F.A., Essumang, D.K., Luginaah, I., Clarke, E., Marfo, K., Cobbina, S.J., Nketiah-Amponsah, E., Namujju, P.B., Obiri, S., Dzodzomenyo, M., 2015. Association of arsenic with adverse pregnancy outcomes-infant mortality: a systematic review and meta-analysis. Environ. Health Perspect. 123, 412–421. https://dx.http://dx.doi.org/10.1289/ehp.1307894.

Qureshi, A., Jia, Y., Maurice, C., Öhlander, B., 2016. Potential of fly ash for neutralisation of acid mine drainage. Environ. Sci. Pollut. Res. 23, 17083–17094. https://dx.http://dx.doi.org/10.1007/s11356-016-6862-3.

Ravengai, S., Love, D., Mabvira-Meck, M., Musiwa, K., Moyce, W., 2005. Water quality in an abandoned gold mining belt, Beatrice, Sanyati Valley, Zimbabwe. Phys. Chem. Earth, Parts A/B/C 30, 826–831. https://dx.http://dx.doi.org/10.1016/j.pce.2005.08.026.

Ritchie, V.J., Ilgen, A.G., Mueller, S.H., Trainor, T.P., Goldfarb, R.J., 2013. Mobility and chemical fate of antimony and arsenic in historic mining environments of the Kantishna Hills district, Denali National Park and Preserve, Alaska. Chem. Geol. 335, 172–188. https://dx.http://dx.doi.org/10.1016/j.chemgeo.2012.10.016.

RMH, 2003. Maximum Permissible Concentration (MPC) of Chemical Substances in the Water of Drinking and Cultural-domestic Water Objects HN 2.1.5.1315-03, 2003. Russian Ministry of Health, Moscow, Russia.

Romero, F.M., Prol-Ledesma, R.M., Canet, C., Alvares, L.N., Pérez-Vázquez, R., 2010. Acid drainage at the inactive Santa Lucia mine, western Cuba: natural attenuation of arsenic, barium and lead, and geochemical behavior of rare earth elements. Appl. Geochem. 25, 716–727. http://dx.doi.org/10.1016/j.apgeochem.2010.02.004.

Roussel, C., Néel, C., Bril, H., 2000. Minerals controlling arsenic and lead solubility in an abandoned gold mine tailings. Sci. Total Environ. 263, 209–219. https://dx.http://dx.doi.org/10.1016/S0048-9697(00.

Saryg-ool, B.Y., Myagkaya, I., Kirichenko, I., Gustaytis, M., Shuvaeva, O., Zhmodik, S., Lazareva, E., 2017. Redistribution of elements between wastes and organic-bearing material in the dispersion train of gold-bearing sulfide tailings: Part I. Geochem. Min. Sci. Total Environ. 581–582, 460–471. https://dx.http://dx.doi.org/10.1016/j.scitotenv.2016.12.154.

Savage, K.S., Tingle, T.N., O'Day, P.A., Waychunas, G.A., Bird, D.K., 2000. Arsenic speciation in pyrite and secondary weathering phases, Mother Lode gold district, Tuolumne County, California. Appl. Geochem. 15, 1219–1244. https://dx.http://dx.doi.org/10.1016/S0883-2927(99.

Savichev, O.G., 2014. Regional peculiarities of chemical composition of Siberian sewage and taking such peculiarities into account in the standardization of sewage disposal. Water Chem. Ecol. 1, 41–46.

Shuvaeva, O.V., Bortnikova, S.B., Korda, T.M., Lazareva, E.V., 2000. Arsenic speciation in a contaminated gold processing tailings dam. Geostand. Geoanal. Res. 24, 247–252. https://dx.http://dx.doi.org/10.1111/j.1751-908X.2000.tb00776.x.

Shvartsev, S.L., Rasskazov, N.M., Savichev, O.G., 1997. Contents and migration forms of elements in natural waters of the Mid-Tom' basin. Rus. Geol. Geophys. 12, 1955.

Sidenko, N.V., Lazareva, E.V., Bortnikova, S.B., Kireev, A.D., Sherriff, B.L., 2005. Geochemical and mineralogical zoning of high-sulfide mine-waste at the Berikul mine-site, Kemerovo region, Russia. Can. Mineral. 43, 1141–1156. https://dx.http://dx.doi.org/10.2113/gscanmin.43.4.1141.

Simmler, M., Suess, E., Christl, I., Kotsev, T., Kretzschmar, R., 2016. Soil-to-plant transfer of arsenic and phosphorus along a contamination gradient in the mining-impacted Ogosta River floodplain. Sci. Total Environ. 572, 742–754. https://dx.http://dx.doi.org/10.1016/j.scitotenv.2016.07.049.

Skousen, J., Simmons, J., McDonald, L.M., Ziemkiewicz, P., 2002. Acid-base accounting to predict post-mining drainage quality on surface mines. J. Environ. Qual. 31, 2034–2044. https://dx.http://dx.doi.org/10.2134/jeq2002.2034.

Smith, A.M.L., Hudson-Edwards, K.A., Dubbin, W.E., Wright, K., 2006. Dissolution of jarosite [$KFe_3(SO_4)_2(OH)_6$] at pH 2 and 8: insights from batch experiments and computational modelling. Geochem. Cosmochim. Acta 70, 608–621. https://dx.http://dx.doi.org/10.1016/j.gca.2005.09.024.

Sobek, A.A., Schuller, W.A., Freeman, J.R., Smith, R.M., 1978. Field and Laboratory Methods Applicable to Overburden and Mine Soils. US EPA 600/2-78-054.

Strosnider, W.H.J., Llanos López, F.S., Nairn, R.W., 2011. Acid mine drainage at Cerro Rico de Potosí I: unabated high-strength discharges reflect a five century legacy of mining. Environ. Earth Sci. 64, 899–910. https://dx.http://dx.doi.org/10.1007/s12665-011-0996-x.

Tolaymat, T., El Badawy, A., Sequeira, R., Genaidy, A., 2015. An integrated science-based methodology to assess potential risks and implications of engineered nanomaterials. J. Hazard Mater. 298, 270–281. https://dx.http://dx.doi.org/10.1016/j.jhazmat.2015.04.019.

Tycholiz, C., Ferguson, I.J., Sherriff, B.L., Cordeiro, M., Sri Ranjan, R., Pérez-Flores, M.A., 2016. Geophysical delineation of acidity and salinity in the Central Manitoba gold mine tailings pile, Manitoba, Canada. J. Appl. Geophys. 131, 29–40. https://dx.http://dx.doi.org/10.1016/j.jappgeo.2016.05.006.

Walker, F.P., Schreiber, M.E., Rimstidt, J.D., 2006. Kinetics of arsenopyrite oxidative dissolution by oxygen. Geochem. Cosmochim. Acta 70, 1668–1676.

Wang, S., Mulligan, C.N., 2006. Occurrence of arsenic contamination in Canada: sources, behavior and distribution. Sci. Total Environ. 366, 701–721. https://dx.http://dx.doi.org/10.1016/j.scitotenv.2005.09.005.

Wei, X., Rodak, C.M., Zhang, S., Han, Y., Wolfe, F.A., 2016. Mine drainage generation and control options. Water Environ. Res. 88 (10), 1409–1432.

Welch, S.A., Kirste, D., Christy, A.G., Beavis, F.R., Beavis, S.G., 2008. Jarosite dissolution II-Reaction kinetics, stoichiometry and acid flux. Chem. Geol. 254, 73–86. https://dx.http://dx.doi.org/10.1016/j.chemgeo.2008.06.010.

WHO, 2011. Background Document for Preparation of WHO Guidelines for Drinking-Water Quality, fourth ed. World Health Organization, Geneva.

Woo, N.C., Choi, M.J., 2001. Arsenic and metal contamination of water resources from mining wastes in Korea. Environ. Geol. 40, 305–311. https://dx.http://dx.doi.org/10.1007/s002540000161.

Yurkevich, N.V., Saeva, O.P., Karin, Y.G., 2015. Geochemical anomalies in two sulfide-bearing waste disposal areas: Fe, Cu, Zn, Cd, Pb, and as in contaminated waters and snow, Kemerovo and Chelyabinsk regions, Russia. Toxicol. Environ. Chem. 97, 76–89. https://dx.http://dx.doi.org/10.1080/02772248.2015.1041955.

Yurkevich, N., Bortnikova, S., Olenchenko, V., Abrosimova, N., Saeva, O., Karin, Y., 2017a. Study of water-rock interaction in sulfide mining tailings using geochemical and geoelectrical methods. Procedia. Earth Planet. Sci. 17, 112–115. https://dx.http://dx.doi.org/10.1016/j.proeps.2016.12.019.

Yurkevich, N.V., Abrosimova, N.A., Bortnikova, S.B., Karin, Y.G., Saeva, O.P., 2017b. Geophysical investigations for evaluation of environmental pollution in a mine tailings area. Toxicol. Environ. Chem. 99 (9–10), 1328–1345. https://doi.org/10.1080/02772248.2017.1371308.

Zarroca, M., Linares, R., Velásquez-López, P.C., Roqué, C., Rodríguez, R., 2015. Application of electrical resistivity imaging (ERI) to a tailings dam project for artisanal and small-scale gold mining in Zaruma-Portovelo. Ecuador. J. Appl. Geophys. 113, 103–113. https://doi.org/10.1016/j.jappgeo.2014.11.022.